



1 **Load-resistance analysis: An alternative approach to tsunami damage assessment applied**
2 **to the 2011 Great East Japan tsunami**

3
4 Anawat Suppasri¹, Kwanchai Pakoksung¹, Ingrid Charvet², Constance Ting Chua³, Noriyuki
5 Takahashi⁴, Teraphan Ornthammarath⁵, Panon Latcharote⁶, Natt Leelawat⁷ and Fumihiko
6 Imamura¹

7
8 ¹International Research Institute of Disaster Science, Tohoku University
9 (468-1 Aramaki-aza Aoba, Aoba-ku, Sendai 980-0845, Japan)

10 ²Department of Statistical Science, University College London, United Kingdom
11 (Gower Street, London, WC1E 6BT)

12 ³Asian School of the Environment, Nanyang Technological University
13 (N2-01C-39, 50 Nanyang Avenue, Singapore 639798)

14 ⁴Department of Architecture and Building Science, School of Engineering, Tohoku University
15 (6-6-11-1 Aramaki-aza Aoba, Aoba-ku, Sendai 980-8579, Japan)

16 ⁵Department of Civil and Environmental Engineering, Faculty of Engineering, Mahidol University
17 (25/25 Puttamonthon, Nakorn Pathom, 73170, Thailand)

18 ⁶Department of Sustainable Development Technology, Faculty of Science and Technology, Thammasat
19 University
20 (99 Moo 18, Phaholyothin Road, Tambon Klong Nung, Amphoe Klong Luang, Pathum Thani 12120,
21 Thailand)

22 ⁷Disaster and Risk Management Information Systems Research Group, Department of Industrial
23 Engineering, Faculty of Engineering, Chulalongkorn University
24 (Phayathai Road, Pathumwan, Bangkok 10330 Thailand)

25
26 **Abstract**

27 Tsunami fragility functions describe the probability of structural damage to tsunami flow characteristics.
28 Fragility functions developed from past tsunami events (e.g. 2004 Indian Ocean tsunami) are often
29 applied directly, without modifications, to other areas at risk of tsunami for the purpose of damage and
30 loss estimations. Consequentially, estimates carry uncertainty due to disparities in construction
31 standards and coastal morphology between the specific region for which the fragility functions were
32 originally derived and the region where they were being used. The main objective of this study is to
33 provide an alternative approach to assessing tsunami damage, especially for buildings in regions where
34 previously developed fragility functions do not exist. A damage assessment model is proposed in this
35 study, where load-resistance analysis is performed for each building by evaluating hydrodynamic forces,
36 buoyancies and debris impacts and comparing them to the resistance forces of each building. Numerical
37 simulation was performed in this study to reproduce the 2011 Great East Japan tsunami in Ishinomaki
38 city, which is chosen as a study site. Flow depths and velocities were calculated for approximately 20,
39 000 wooden buildings in Ishinomaki city. Similarly, resistance forces (lateral and vertical) are estimated
40 for each of these buildings. The buildings are then evaluated for its potential to collapse. Results from
41 this study reflect a higher accuracy in predicting building collapse when using the proposed load-
42 resistance analysis as compared to previously developed fragility functions in the same study area.
43 Damage is also observed to have likely occurred before flow depth and velocity reach maximum values.
44 With the above considerations, the proposed damage model might well be an alternative for building
45 damage assessments in areas which have yet to be affected by modern tsunami events.

46

47 **Figures with higher quality can be seen in supplemental file.**

48

49



50 1. Introduction

51 The 2011 Great East Japan earthquake generated a large tsunami which damaged and destroyed more
52 than 250, 000 buildings (MLIT, 2012). Building damage characteristics from the 2011 event have since
53 been well-studied and in most cases, used to develop tsunami damage fragility functions (Suppasri et
54 al., 2015). Tsunami damage fragility functions describe the probability of structural damage to tsunami
55 flow characteristics, i.e. flow depth, flow velocity and hydrodynamic force. Fragility functions have
56 been developed from past events (e.g. 2004 Indian Ocean, 2010 Chile and 2011 Great East Japan
57 tsunamis) and are often applied directly, without modifications, to other areas facing tsunami risk for
58 damage and loss assessments (Suppasri et al., 2016). The resulting damage estimates carry uncertainty
59 related to differences in construction standards and coastal morphology between the specific region for
60 which the fragility functions were originally derived and the region where they are being used.

61 Tsunami fragility functions are modelled using tsunami flow characteristics and building damage
62 information. These characteristics are usually obtained through either: – 1) Field survey and 2)
63 Combined analyses from tsunami numerical simulation and satellite imagery (Charvet et al, 2017). In a
64 field survey, maximum flow depth measured from tsunami water traces are typically used as
65 explanatory variables of damage. Building damage data is obtained from on-site observations (Reese et
66 al., 2007, Valencia et al., 2011, Suppasri et al., 2015 and Triantafyllou et al., 2018). This method
67 combines tsunami numerical simulation, which generates maximum flow depth, flow velocity and
68 hydrodynamic force values, and satellite image analysis of pre- and post- disaster images to obtain
69 building damage data (Koshimura et al., 2009, Omira et al., 2010 and Suppasri et al., 2011) or other
70 damage data set such as damaged marine vessels (Suppasri et al., 2014), damaged bridges (Shoji and
71 Nakamura, 2017) as well as aquaculture rafts and eelgrass (Suppasri et al., 2018). In both methods, only
72 maximum values of tsunami flow characteristics are considered as explanatory variables. However, a
73 given damage level might have already occurred before these maximum values are attained, thus
74 building damage may be underestimated. Additionally, recent studies have shown tsunami
75 hydrodynamic force to be an important explanatory parameter (Macabuag et al., 2016), flow velocity
76 at time of occurrence (Song et al., 2018) and floating debris (Macabuag et al., 2018) are all factors when
77 assessing building damage.

78 In order to obtain fragility functions for areas where tsunami data is not yet available, it is necessary to
79 model the deterministic processes relating tsunami characteristics to the capacity of the structure to
80 resist resulting loads. This allows for the structural characteristics information specific to the buildings
81 of a region to be taken into account, as well as bypassing the use of potentially biased observed values
82 for the explanatory variables. This study investigates interactions between tsunami loading and the
83 resistance of a system (in this case the resistance of a building) through an analytical model to infer
84 tsunami damage. The objective is to provide an alternative approach to assessing tsunami damage
85 especially for buildings in areas where previously developed fragility functions do not exist. As part of
86 this study, tsunami characteristics at the time of damage occurrence will be investigated and used in the
87 proposed model to provide a complementary insight into the relationship between structural damage
88 and tsunami flow characteristics.

89 The analytical model is defined following an overview of tsunami flow characteristics and their effects
90 on buildings. Next, the study site and building damage data set used to demonstrate the application of
91 the model are presented. Two major components of the model are then discussed: tsunami numerical
92 simulation and the estimation of resisting forces. Model results are compared to other building damage
93 assessment estimates and observations in order to examine their applicability in building damage
94 estimation. In addition, because structural damage is usually presented in a qualitative manner, most
95 tsunami damage assessments may not be readily usable by private or governmental organisations.
96 Therefore, a financial metric converting existing structural damage levels into financial cost ratios is
97 proposed.



98

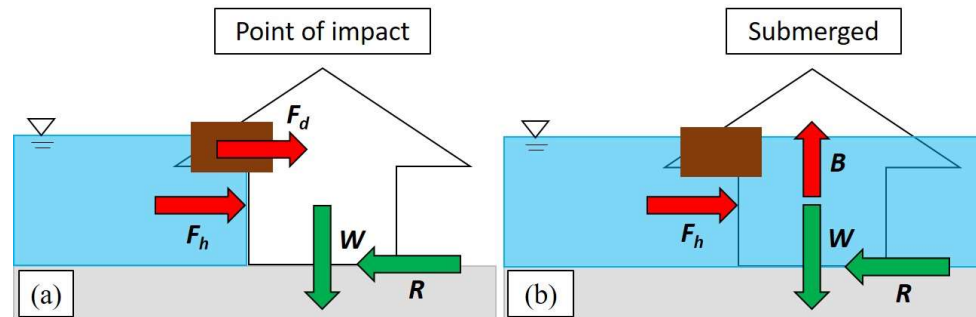
99 **2. Alternative approach to tsunami damage assessment**

100 Damage by tsunamis to infrastructure are caused by many factors such as tsunami forces, impact of
101 waterborne debris, building characteristics and scouring of foundations (Kelman and Spence, 2004).
102 Forces generated by a tsunami can be estimated by classifying them according to their flow conditions
103 and characteristics. Hydrodynamic force is generated by the pressure from flowing waters around the
104 structure, and is influenced by flow velocity, depth and density of the water as well as the geometry and
105 angle at which the tsunami hits the structure (Nadal et al., 2010). When hydrodynamic force is used in
106 tsunami science, it usually refers to the drag force which is directly proportional to the square of flow
107 velocity. Debris impact force is driven by tsunami flow. Tsunami-borne debris, while not a direct action
108 of tsunami flow, can cause substantial damage to buildings. It can result in the reduction of load-bearing
109 capacity in a building, and therefore the reduction in structural resistance to lateral loads and buoyancy
110 forces (Nadal et al., 2010).

111 The approach taken in this study is an adaptation from Latcherote et al (2017) where they analysed and
112 compared the overturning mechanism with resisting moment for six overturned reinforced concrete
113 buildings in Onagawa town. Similarly, the proposed damage model performs load-resistance analysis
114 for each building by evaluating hydrodynamic forces, buoyancy forces and debris impacts and
115 comparing them to the resistance of each building. There are two general types of resistance that a
116 building provides. First, it provides lateral resistance which is designed to counter loads that are
117 perpendicular to and imposed on walls. Second, the weight of the buildings acts as downward-acting
118 (vertical) resistance against buoyancy forces or upward-acting loads from wind and seismic activities.
119 The resistance force from pile foundation was also one of the components examined Latcherote et al.
120 (2016). However, because wooden buildings were used for this study, the resistance force from pile
121 foundation was not considered.

122 Global stability failure in a building can be a result of either sliding or overturning as a solitary body,
123 often with minimal damage to structural/non-structural components (Yeh et al, 2014). Overturning
124 refers to the rotation of a building about its foundation where it has failed. Sliding, on the other hand,
125 is the horizontal translation of a building from its original position (Yeh et al, 2014). The two
126 mechanisms are modelled separately in this study to determine the predominant mechanism for building
127 collapse. Differences in the forces and resistance involved in these mechanisms were considered when
128 performing load-resistance analysis:

- 129 (1) Sliding/Non-submerged at the point of impact (**Fig. 1 (a)**): Only horizontal hydrodynamic force,
130 debris impact and lateral resistance of the building were considered in this case. A building
131 collapses if the compounded hydrodynamic and debris impact forces are greater than the lateral
132 resistance of the building.
- 133 (2) Overturning/Submerged (**Fig. 1 – (b)**): A building collapses when the overturning moment
134 from hydrodynamic and buoyancy forces is greater than the resisting moment from the building
135 weight. Under such circumstances, the building can either be fully submerged as illustrated in
136 **Fig. 1 (b)** or surrounded by water with no water inside. In the former case, when the building
137 is completely inundated, forces from the exterior of the building are cancelled out. The latter is
138 the worst-case scenario and is assumed for subsequent analyses of overturning mechanisms in
139 this study.



140

141

Fig.1 Two failure mechanism considered in this study: (a) Sliding and (b) overturning.

142

143

2.1 Selection of study site

144

145

146

147

148

There were many possible areas for studying building damage from the 2011 Great East Japan tsunami event. A suitable study site needs to be highly representative of the processes being modelled, without excessive contributions of un-modelled effects. In addition, a previously investigated area would allow for a fair assessment of the analytical model's results. Ishinomaki City, Miyagi Prefecture was therefore selected as the area displayed the following characteristics:

149

150

151

152

153

154

155

156

157

158

159

160

161

162

163

1. Less impact from wave amplification: Ishinomaki City is located on a plain coast which reduces the effects of wave amplification unlike coastal towns located along the Sanriku Ria Coast
2. Less impact from floating debris: The populated areas of Ishinomaki are far from fishing ports and storage facilities, many of which were damaged by the tsunami and generated floating debris, which can magnify building damage. Floating debris from broken pine trees can also be excluded from consideration as the coastal pine forest along the city survived.
3. Less impact from wave directions: The effects from varying wave directions are minor as most of the buildings were lined facing the shoreline and the direction of wave attack was perpendicular to the front of the buildings.
4. Largest sample size: The number of buildings affected by the 2011 event was largest in Ishinomaki City amongst cities along the plain coast.
5. Previously developed fragility functions: Fragility functions have been previously developed for the populated areas of Ishinomaki City (Charvet et al., 2014). A new study from Hasegawa et al., (2018) provides an excellent opportunity to compare the proposed method in this study with the established model.

164

2.2 Building damage data

165

166

167

168

169

170

171

172

173

174

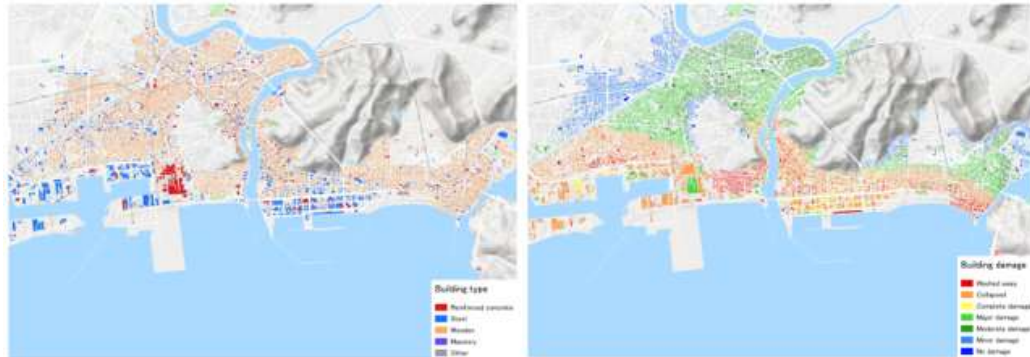
175

176

177

178

Detailed building damage data from field observations was obtained from the Ministry of Land, Infrastructure and Transportation and Tourism (MLIT) (MLIT, 2012) (**Fig. 2**) to test the applicability of the proposed building damage model. The data consists of building size (length and width), number of stories, construction material and interpolated measured maximum flow depth of each building. Each building was also classified according to their observed damage. There are a total of six damage levels in the classification scheme by MLIT. Low damage levels (i.e. levels 1 – 4) are easily misclassified in damage assessments due to overlapping descriptions in the classification scheme (Leelawat et al., 2014), whereas damage levels 5 and 6 are straightforward in their definitions (**Fig. 3**). “Washed away” and “destroyed” (levels 5 and 6) refer to structures which are irreparable. In this study, the two levels “washed away” and “destroyed” are considered since sliding and overturning mechanisms fall into the aforementioned categories. As opposed to lower damage levels, these damage modes are driven by the structural properties of these buildings, thus only buildings damaged at these levels were used for this study. The building type considered in this pioneer study is only wooden residential houses due to their large sample size in this area.



179
180 **Fig.2** (Left) Distributions of building types and (Right) building damage levels.
181



182
183 **Fig. 3** Building damage levels and collapsed condition considered in this study.
184

185 2.3 Numerical simulation of the 2011 tsunami and damage inducing forces

186 Tsunami flow characteristics (flow depth, velocity and hydrodynamic force) at the point of damage
187 occurrence were estimated in a time series analysis of the 2011 Great East Japan tsunami, which was
188 reproduced by numerical simulation. The numerical model computed tsunami propagation and run-up
189 by using a set of nonlinear shallow water equations which were solved by staggered leap-frog finite
190 difference scheme, and bottom frictional values were written using Manning's formula (Suppasri et al.,
191 2011, Charvet et al., 2015 and Macabaug et al., 2016). The model set-up includes the preparation of
192 bathymetry and topography data – a nested grid system consisting of six computational domains – 1215
193 m (Region 1), 405 m (Region 2), 135 m (Region3), 45 m (Region 4), 15 m (Region 5) and 5 m (Region
194 6) was used for the study area (**Fig. 4**). Only at the finest resolution (Region 6) were different Manning's
195 roughness coefficients specified according to land use types and building density, as the effect of
196 bottom friction on tsunami propagation in deep waters negligible. Tidal level was set to tide conditions
197 at the time of tsunami occurrence, and simulation time was set to three hours. Initial water surface
198 elevation was assumed to follow sea floor deformation, the fault parameters proposed by Tohoku
199 University model (Imamura et al, 2016) were selected to reproduce the 2011 Great east Japan tsunami.
200 Results of numerical simulation are shown in **Fig. 5**.

201 The accuracy of model is validated by comparing measured tsunami trace heights and modelled results
202 (**Fig. 6**) using Aida's K and κ (Aida, 1978) as defined in equations (1) - (3) below.



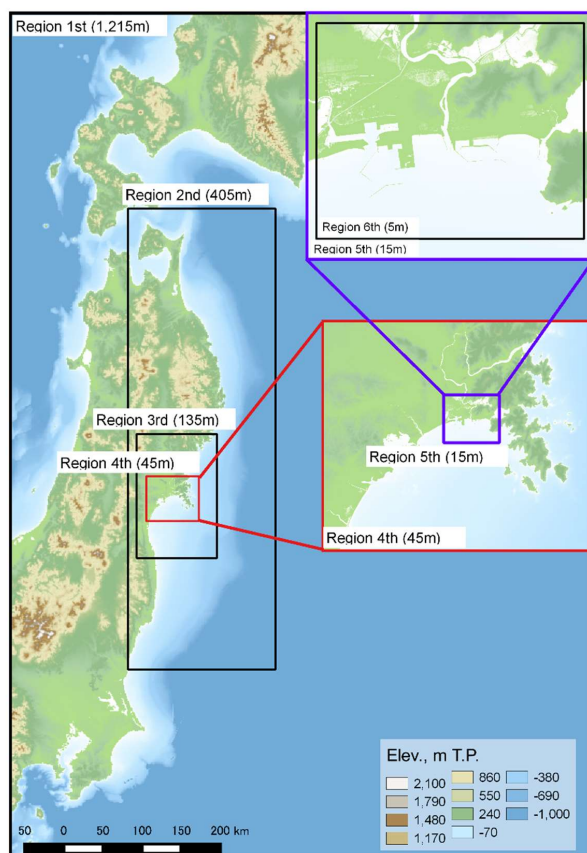
203
$$\log K = \frac{1}{n} \sum_{i=1}^n \log K_i \quad (1)$$

204
$$\log \kappa = \sqrt{\frac{1}{n} \sum_{i=1}^n (\log K_i)^2 - (\log K)^2} \quad (2)$$

205
$$K_i = \frac{x_i}{y_i} \quad (3)$$

206

207 Where, x_i and y_i are the measured and simulated tsunami trace heights (Mori et al., 2012) at point i .
 208 Consequently, K is regarded as a correction factor to adjust the modeled values to fit the actual tsunami
 209 averaged over several locations; κ is defined as a measure of the fluctuation or deviation in K_i . Values
 210 of Aida's K and κ are 1.04 and 1.32 respectively. The corrected tsunami simulation produced tsunami
 211 flow depths which are a close match to the measured tsunami trace heights and satisfy the guideline of
 212 the Japan Society of Civil Engineers (JSCE) ($0.95 < K < 1.05$ and $\kappa < 1.45$) (JSCE, 2016). Hence,
 213 tsunami flow depths and velocities in Ishinomaki City of higher accuracy were reproduced.

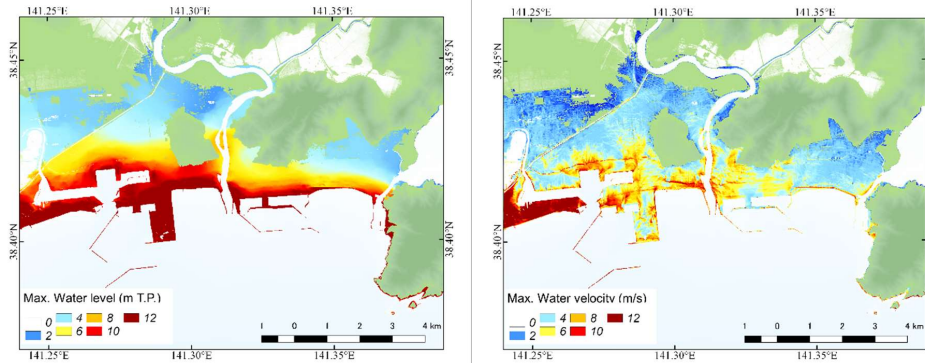


214
 215

Fig.4 Computational regions in this study.



216



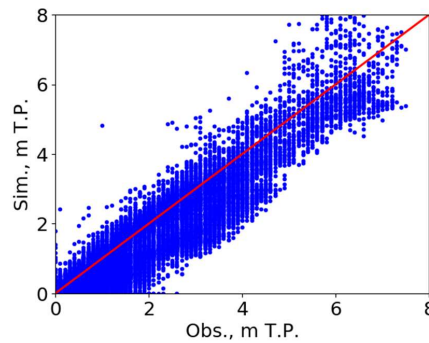
217

218

219

220

Fig. 5 Results of tsunami numerical simulation: (Left) Maximum flow depth and (Right) Maximum flow velocity.



221

222

223

224

Fig. 6 Validation of the simulated tsunami inundation heights using the observed tsunami trace heights (Mori et al., 2012).

225

226

227

228

229

230

Results from the tsunami simulation were used to estimate tsunami-induced forces. Flow depth and velocity values were captured at each time step of the simulation and at each building location for more than 20,000 wooden buildings in Ishinomaki city. These values were then used to calculate hydrodynamic force (F_h) through drag formula (equation (4)), debris impact force (F_d) through impulse-momentum approach (equation (5)) as well as buoyancy force (B) (equation (6)) at each time step for each building (**Fig. 1**).

231

$$F_h = \frac{1}{2} C_D \rho u^2 D \quad (4)$$

232

233

$$F_d = m \frac{u}{\Delta t} \quad (5)$$

234

235

$$B = \rho g V \quad (6)$$

236

237

238

Where C_D denotes the drag coefficient ($C_D = 1.5$), ρ the density of water ($= 1,000 \text{ kg/m}^3$), u the current velocity (m/s), D inundation depth (m), m (kg) the weight of debris, Δt the duration of impact ($= 0.7 \text{ sec}$)



239 for wooden wall), g the gravitational acceleration and V the submerged volume. This study follows the
240 recommended weights of floating debris by the American's Federal Emergency Management Agency
241 (FEMA, 2003) and Japan Society of Material Cycles and Waste Management (JSCWM, 2011), where
242 the estimates were approximately 500 kg for a pine tree, 3,000 kg for a vehicle, and buildings - 15,000
243 kg, 30,000 kg and 60,000 kg for moderately damaged, majorly damaged and collapsed buildings
244 respectively.

245

246 **2.4 Resistant forces**

247 In this study, the designed resistance of each building to withstand loads imposed on them is considered
248 as its damage threshold. One aim is to determine if the modelled tsunami induced forces (i.e.
249 hydrodynamic force, buoyancy force and debris impact force) for each building would exceed its
250 damage threshold and therefore, result in damage to the building. As mentioned earlier, differences in
251 the types of loads imposed and types of building resistance forces involved were considered when
252 modelling sliding and overturning mechanism of a building. Both mechanisms were modelled
253 separately. There are two types of resistant forces in a building i.e. vertical and lateral resistance. The
254 vertical resistance of a building is its weight, and in this study, it was assumed to be 3,000 kN/m² for
255 each building (Yokohama City, 2018). Vertical load-resistance analysis was used to determine
256 overturning mechanisms.

257 For the first time, lateral resistance (R) from the bearing wall of a building will be considered when
258 estimating building damage from tsunamis. The failure of lateral resistance of a building can imply that
259 sliding mechanisms are involved in its collapse. The bearing wall of a building must be able to resist
260 lateral loads imposed on them such as wind or seismic activity. The lateral resistance of each building
261 to earthquake and wind forces was calculated in accordance with Article 46 Enforcement Ordinance of
262 Building Standard Law (MLIT, 2018), and in which case, lateral resistance is the product of the lateral
263 strength of the bearing wall and the required wall length of each building. The lateral strength of the
264 bearing wall by Japanese housing design standard is 1.96 kN/m (MLIT, 2018).

265 Calculations for the required wall length would differ for both seismic and wind loads. Required wall
266 length for seismic loads can be derived by taking the building's floor area and multiplying it by its
267 design coefficient for seismic load (**Fig. 7**) as illustrated in Example 1. On the other hand, for wind
268 loads, the required wall length can be calculated by multiplying the design coefficients with the vertical
269 projection area (both the front and side of the building) as illustrated in Example 2. The vertical
270 projection area is the area defined by the building width or length multiplied by the floor height above
271 1.35 m (**Fig. 8**). As information on building heights in Ishinomaki city was not available at the point of
272 this study, 3.5 m, 2.7 and 2.1 m were assumed to be the heights of the first, second and third floors
273 respectively. Wooden buildings in Ishinomaki city did not exceed three stories.

274 In this study, the lateral resistance of a building against tsunami impacts is considered as the sum of
275 lateral resistance for floors below the modelled maximum flow depth. Estimation of lateral resistance
276 for buildings should be taken with care as it was calculated for each floor. The total lateral resistance of
277 a building against seismic or wind loads would be the sum of lateral resistance for every floor where
278 maximum tsunami flow depth has reached. The highest estimated lateral resistance between seismic
279 and wind loads was then chosen as the maximum effective resistance, hence the assumed lateral
280 resistance design for each building. It should also be noted that the design lateral resistance may
281 decrease due to age and ground shaking from previous earthquakes. A previous study done by the Japan
282 Building Disaster Prevention Association (2012) reported 0.7 as the minimum reduction coefficient to
283 account for these effects. Therefore, a range of bearing wall resistance reduction coefficients (0.7, 0.8,
284 0.9 and 1.0) was introduced when calculating the lateral resistance of the building.

285

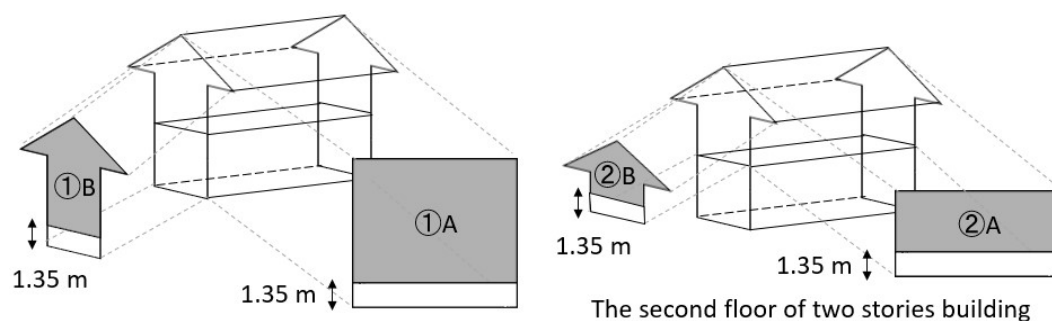


286 **Example 1**
 287 Calculation example of required wall length for seismic load
 288 One story with 60 m² of floor area, the required wall length = 60 m² × 15 cm/m² = 900 cm = 9 m
 289
 290 **Example 2**
 291 Calculation example of required wall length for wind load
 292 The first floor of two stories building,
 293 Front: Required wall length = ①A (m²) × 50 cm/m²
 294 Side: Required wall length = ②B (m²) × cm/50 m²
 295
 296 The second floor of two stories building
 297 Front: Required wall length = ②A (m²) × 50 cm/m²
 298 Side: Required wall length = ②B (m²) × cm/50 m²
 299 The design wall length for wind load will be the summation of the maximum value at each floor.
 300

15 cm/m ²	One story building
33 cm/m ²	The first floor of two stories building
21 cm/m ²	The second floor of two stories
50 cm/m ²	The first floor of three stories building
39 cm/m ²	The second floor of three stories building
24cm/m ²	The third floor of three stories building

301
 302
 303
 304
 305

Fig. 7 Design coefficients for calculating corresponding necessary wall length against seismic load for 1-3 stories wooden houses.



306

The first floor of two stories building

307

Fig. 8 Calculation example of corresponding necessary wall length against wind load.

308

309 2.5 Building damage replacement cost ratio

310 Although financial loss is not the central focus of this paper, it is a good opportunity to present a
311 potential building damage replacement cost index for wooden buildings for future loss estimates. At
312 present, tsunami building damage costs are based on data obtained from insurance claims after tsunami
313 events. Loss estimates are, for the most part, based on analyses which are separate from the damage
314 assessments and they do not account for building conditions and tsunami hydrodynamics.

315 The building damage levels proposed by MLIT (**Fig. 3**) formed the basis of developing the replacement
316 cost index. Throughout this study, the focus has been on collapsed buildings (levels 5 and 6). This index
317 however will be representative of both collapsed and non-collapsed buildings. Collapsed buildings can
318 automatically be assigned as 100% loss as they are assumed to be irreparable. In general, construction
319 costs of two-storey wooden houses in Japan comprise two components – architectural works which
320 forms 70% of total costs and structural works which forms 30%. Costs of structural works can be further
321 broken down into non-structural components (roofs (20%) and walls (10%)) and structural components
322 (beams (20%), columns (15%) and footings (45%)) of the building. The averaged numbers of each
323 component were calculated based on actual data of several houses (MN Housing and Building
324 Laboratory, 2015, Cabinet Office of Japan, 2017, and Japan Wood-Products Information and Research
325 Center, 2019.).

326

327 3. Results and discussion

328 3.1 Accuracy of the proposed building damage assessment method

329 The results of the proposed building damage assessment model were compared to field observations to
330 assess its performance (**Fig. 9**). Field observations are presented in the MLIT database and only
331 buildings with damage levels 5 and 6 (collapse conditions) were used for comparison. **Table 1** shows
332 an accuracy of modelled collapsed buildings and actual collapsed buildings from field observations
333 when only sliding mechanism was considered, and **Table 2** when both sliding and overturning
334 mechanisms were considered. Both tables have clearly illustrated that debris impact forces and
335 resistance reduction coefficients do not seem to have significantly influenced the collapse of buildings
336 in Ishinomaki. Damage analysis without debris weight input and building resistance reduction
337 coefficient showed a better match. This can be attributed to the fact that Ishinomaki city was not heavily
338 affected by floating debris for the reasons stated in **section 3.1**.

339

340 **Tables 3** and **4** highlight sliding mechanism alone is a poor explanation of collapse. In other words,
341 overturning is an important mechanism when analyzing building collapse. When using the proposed



342 method, the modelled results show a near 100% accuracy, as shown in **Table 4** and illustrated in **Fig.**
 343 **9**.

344 **Table 1** Damage assessment accuracy (%): Washed away and destroyed buildings (damage levels 5
 345 and 6) by considering only sliding as damage mechanism.

Debris weight	Resistance reduction coefficient			
	1	0.9	0.8	0.7
0 ton	65.24	66.54	68.02	69.84
0.5 tons	59.27	60.44	61.86	63.61
3 tons	61.43	62.92	64.55	66.39
15 tons	67.45	68.88	70.56	72.26
30 tons	72.44	72.21	71.13	69.43
60 tons	89.32	89.40	89.49	59.48

346

347 **Table 2** Damage assessment accuracy (%): Washed away and destroyed buildings (damage levels 5
 348 and 6) by considering both damage mechanisms.

Debris weight	Resistance reduction coefficient			
	1	0.9	0.8	0.7
0 ton	99.79	99.77	99.73	99.69
0.5 tons	96.46	96.44	96.40	96.35
3 tons	96.29	96.19	96.03	95.81
15 tons	91.97	91.25	90.17	88.96
30 tons	85.37	83.71	81.67	79.49
60 tons	93.73	93.77	93.83	72.26

349



350

351 **Fig. 9** Distributions of collapsed and non-collapsed buildings from field observation (left) and the
 352 proposed method (right)

353 3.2 Comparison of minimum load values for the collapse of wooden buildings against field 354 observations and hydraulic experiments

355 The average lateral resistance of a building in Ishinomaki, derived from 19,000 wooden houses in this
 356 study, is estimated to be about 42 kN, and the average hydrodynamic force is about 10 kN. These
 357 findings are evaluated and compared to other findings in tsunami literature to understand the dominant
 358 mechanism of building collapse. In a hydraulic experiment by Arikawa (2009), the flexural capacity of
 359 a wooden wall was tested. A wooden wall (2.5 m high and 2.7 wide) supported by a steel frame was
 360 placed in a water flume in a full-scale experiment. The wooden wall was found to be destroyed at a



361 tsunami flow depth of 2.5 m. The flexural capacity of the wooden wall was 10 kN/m², which is
362 equivalent to 67.5 kN. Matsutomi and Harada (2010) measured tsunami flow depth at the front and back
363 of buildings during their field survey. Based on the survey and estimated Froude number, they found
364 that for wooden houses, the necessary lateral force required to cause moderate damage is 5.4 – 9.9 kN/m
365 and for major damage, 9.7 – 17.6 kN/m. Therefore, the minimal lateral load required for wooden houses
366 to be washed away is approximately 9.7 – 17.6 kN/m or 88 -176 kN, assuming that the width of the
367 house is 5 – 10 m. This information further supports the consideration of overturning as a critical
368 explanation for collapse mechanism.

369

370 **3.3 Tsunami characteristics at the time of collapse and influence of flow characteristics on** 371 **damage**

372 Critical flow depth (D_c) and critical flow velocity (V_c) values are flow depths and velocities at the time
373 of building collapse or rather, when buildings were considered collapsed when using the proposed
374 damage model. In this study, a further assessment was made to derive maximum flow values and
375 compare them to the critical values modelled for each building. In general, the critical values are lower
376 than maximum values for both flow depth and velocity (**Figs. 10 & 11**). The maximum flow depth (D_m)
377 is about four times higher than the critical flow depth and maximum flow velocity (V_m) is about two
378 times higher than the critical flow velocity (**Table 3**). The implication is straightforward – building
379 damage would be highly underestimated when using maximum flow characteristics as explanatory
380 variables. It underscores one of the weaknesses of using traditional tsunami damage assessment
381 methodologies.

382 It is also observed that flow depth and flow velocity contribute differently to total building damage.
383 Critical flow depth and velocity for collapsed (damage levels 5 and 6) and non-collapsed buildings are
384 plotted in **Fig. 12** and it appears that wooden buildings would almost always get washed away when
385 critical flow velocity exceeds 2 m/s, regardless of the value of critical flow depth. This value may serve
386 as a simple indicative criterion to assess building damage potential. This criterion when used together
387 with developed tsunami maps or numerical flow simulation allows for some initial building damage
388 assessment and quick estimations.

389 The influence of flow depth and flow velocity on building damage may also vary across space. The
390 relationship between critical and maximum flow depth values are represented as ratios and the
391 distribution of these ratios are plotted in a map (**Fig. 13 (Left)**). Similarly, the distribution of the ratio
392 between critical and maximum flow velocities are plotted in a map (**Fig. 13 (Right)**). Flow velocity
393 appears to be a more significant parameter of damage (as ratios are close to 1.00) in areas nearer to the
394 shoreline where flow velocity is very high and tsunami induced force is mostly hydrodynamic. On the
395 other hand, flow depth has a greater influence on damage in areas nearer to the inundation limit where
396 pressure from the tsunami is mostly hydrostatic.



397
 398
 399



Fig. 10 Distribution of the critical flow depth (left) and the maximum flow depth (right)

400
 401
 402

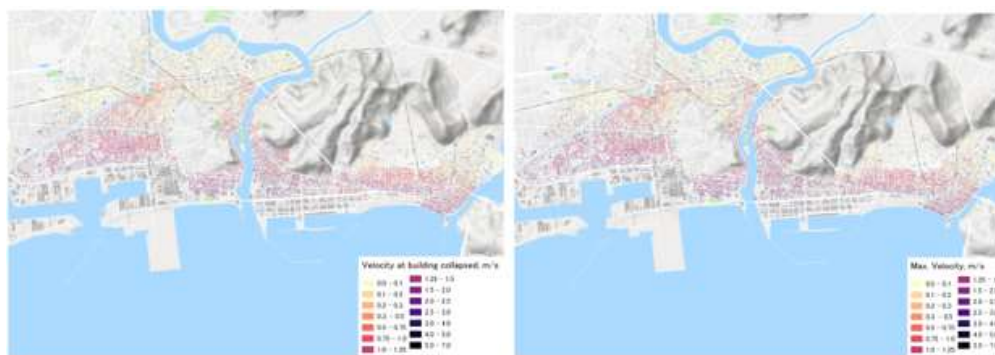
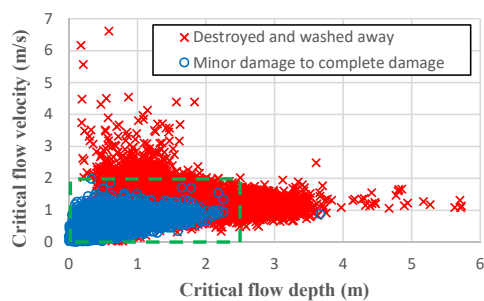


Fig. 11 Distribution of the critical flow velocity (left) and the maximum flow velocity (right)

Table 3 Flow depth and velocity ratios (washed away and destroyed buildings: damages levels 5 and 6).

Damage conditions	D_m / D_c	V_m / V_c
Collapsed	4.03	2.34
Non-collapsed	1.56	1.16

405

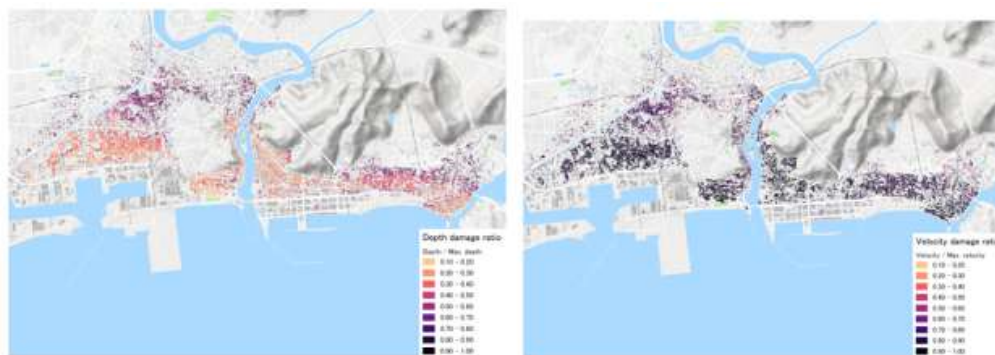


406
 407

Fig.12 Plotting of the critical flow depth and critical flow velocity



408



409

410 **Fig. 13** Distributions of ratios between the critical and the maximum values of the simulated flow
 411 depth (left) and flow velocity (right). Higher ratios are found near inundation limit for the flow depth
 412 whereas near shoreline for the flow velocity.

413

414 3.4 Comparing results from fragility functions

415 Building collapse in Ishinomaki City was recently modelled by Hasegawa et al. (2018), where they
 416 developed fragility functions using the same building damage dataset (MLIT, 2012) and collapse
 417 criteria. The fragility functions were developed by applying logistic regression (where damage states
 418 follow a binomial distribution). The estimated damage probabilities are calculated as per equation (7).
 419 Values of the maximum likelihood estimations are presented in **Table 4**.

420

$$421 \quad p = \frac{1}{1 + \exp(-a_0 - a_i x_i - \dots)} \quad (7)$$

422

423 Where p is a probability of collapse, a_n is a regression constant and x_n is an explanatory variable. In the
 424 damage assessment of this study, a building is classified as collapsed when the probability of collapse
 425 is higher than 50%.

426 **Table 4** The maximum likelihood estimates (Hasegawa et al., 2018)

	Estimate	Stand. Error	Z value	Pr (> z)	
Constant term	-3.9250	0.0514	-76.4360	< 2e-16	***
RC building	-1.7970	0.0814	-22.0870	< 2e-16	***
Wooden building	1.4120	0.0440	32.1180	< 2e-16	***
Numbers of stories	-0.4242	0.0164	-25.8550	< 2e-16	***
Functions	0.2272	0.0277	8.2050	2.31E-16	***
Flow depth	1.0530	0.0060	174.1830	< 2e-16	***
Building area	-0.0003	0.0000	-7.1890	6.53E-13	***

427 p value: *** > 0.001, ** > 0.01, * > 0.05 and . > 0.1

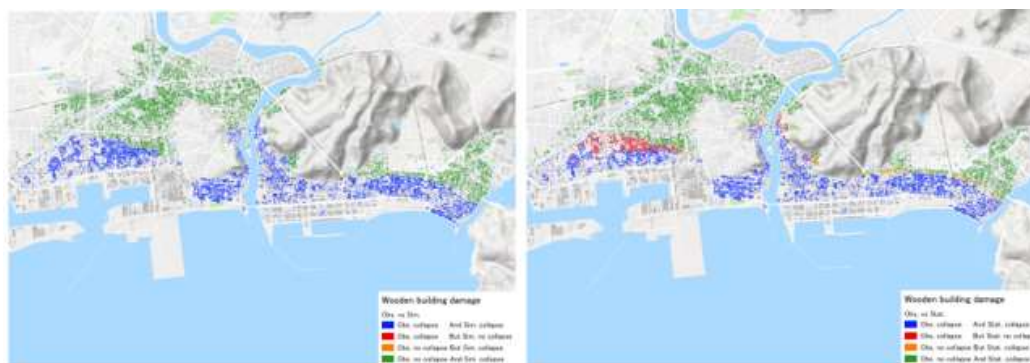
428



429 Results from this study are compared to the fragility functions to determine how well building damage
430 can be identified when using either the proposed method or the fragility functions. The building damage
431 condition is reproduced using both methods and compared to actual observations as shown in **Fig. 14**.
432 The proposed method is able to correctly reproduce collapsed and non-collapsed buildings with 99.79%
433 accuracy, while the fragility functions are able to reproduce building damage conditions with 91.06%
434 accuracy, as summarized in **Table 5**. It can be observed the model based on fragility functions does not
435 perform as well when assessing building damage in the zone separating collapsed and non-collapsed
436 buildings.

437 It should be noted that building damage assessment with such accuracy can only be replicated because
438 of the strict construction design standards in Japan. How well the proposed method will perform in a
439 context outside of Japan will be largely dependent on local practices in the design and construction of
440 the buildings, the presence debris material and the age of the building (resistance reduction coefficients).
441 Additionally, flow-building interactions which yield lower damage states are not accounted for, so the
442 model may not perform as well for flow conditions which are less severe than the 2011 Great East Japan
443 tsunami.

444



445

446 **Fig. 14** Reproduction of building damage condition (collapse or non-collapse): 1) Comparison between
447 the proposed method and field observation and 2) Fragility functions and field observation. Green:
448 Correct reproduction of collapsed buildings, Blue: Correct reproduction of non-collapsed buildings,
449 Red: Failed to reproduce collapsed buildings and Orange: Failed to reproduce non-collapsed buildings.

450

451

452

453

454

455

456

457

458



459 **Table 5** Building damage assessment accuracy of this proposed method and previously developed
 460 fragility functions compared to field observations. This table shows numbers of buildings for each
 461 condition and their accuracy percentages.

462

		Analytical method (this study)	
		Collapsed	Non-collapsed
Field observation	Collapsed	8,518 (45.22%)	33 (0.18%)
	Non-collapsed	7 (0.04%)	10,277 (54.56%)

		Fragility functions	
		Collapsed	Non-collapsed
Field observation	Collapsed	7,362 (39.09%)	1,189 (6.31%)
	Non-collapsed	519 (2.76%)	9,765 (51.85%)

463

464 3.5 Financial loss metrics

465 On account of these approximations of the construction cost, each building damage level defined by
 466 structural damage condition can be converted to replacement cost ratio as follows (see also **Table 6**).

467

468 Damage level 1: Minor damage (Replacement cost ratio = 18%)

469 Because of its damage description as “no significant structural or non-structural damage, possibly only
 470 minor flooding”. A 25% architectural works is applied as the condition “Possible to be use immediately
 471 after minor floor and wall clean up”.

472

473 Damage level 2: Moderate damage (Replacement cost ratio = 36%)

474 A damage ratio of 10% is assigned to roof and wall according to the damage description “Slight
 475 damages to non-structural components”. A 50% architectural works is applied as the condition
 476 “Possible to be use after moderate repair”.

477

478 Damage level 3: Major damage (Replacement cost ratio = 54%)

479 A damage ratio of 25% is assigned to roof and wall according to the damage description “Heavy
 480 damages to some walls but no damages in columns”. A 75% architectural works is applied as the
 481 condition “Possible to be use after major repair”.

482

483 Damage level 4: Complete damage (Replacement cost ratio = 76%)

484 A damage ratio of 50% is assigned to roof and wall and 25% to beam and column according to the
 485 damage description “Heavy damages to several walls and some columns”. A 100% architectural works
 486 is applied as the condition “Possible to be use after a complete repair and retrofitting”.

487

488 Damage level 5: Collapsed (Replacement cost ratio = 100%)

489 A damage ratio of 75% is assigned to roof and wall and 50% to beam and column according to the
 490 damage description “Destructive damage to walls (more than half of wall density) and several columns
 491 (bend or destroyed). However, because a damage ratio of 100% is assigned to footing because of the



492 damage condition “Non-repairable or great cost for retrofitting”, the final replacement cost ratio is set
 493 to 100%.

494

495 Damage level 6: Washed away (Replacement cost ratio = 100%)

496 A damage ratio of 100% is assigned to all structural components according to the damage description
 497 “Washed away, only foundation remained, total overturned” and damage condition “Non-repairable,
 498 requires total reconstruction”.

499

500 **Table 6** MLIT’s damage level classification, description and condition (MLIT, 2012) and the
 501 converted cost replacement ratios

Damage level	Classification	Description	Condition	Replacement ratio
1	Minor damage	There is no significant structural or non-structural damage, possibly only minor flooding	Possible to be use immediately after minor floor and wall clean up	18%
2	Moderate damage	Slight damages to non-structural components	Possible to be use after moderate reparation	36%
3	Major damage	Heavy damages to some walls but no damages in columns	Possible to be use after major reparation	54%
4	Complete damage	Heavy damages to several walls and some columns	Possible to be use after a complete reparation and retrofitting	76%
5	Destroyed or collapsed	Destructive damage to walls (more than half of wall density) and several columns (bend or destroyed)	Loss of functionality (system collapse). Non-repairable or great cost for retrofitting	100%
6	Washed away	Washed away, only foundation remained, total overturned	Non-repairable, requires total reconstruction	100%

502

503 4. Conclusions

504 This study presented a novel quantitative tsunami damage prediction approach, load-resistance analysis.
 505 While previous empirical and experimental studies have vastly improved our understanding of building
 506 response to tsunami impacts and extensively quantified building damage characteristics, implementation
 507 of the resulting damage estimates for future tsunami scenarios is challenging; in particular, when
 508 spatial differences such as construction standards and coastal morphology are significant. Load-
 509 resistance analysis utilizes building design standards to estimate the resistance force of each
 510 building, hence analytically estimate the potential for building damage (collapse) in a localized
 511 context. One of the advantages of load-resistance analysis is it can be extended to other areas
 512 where existing empirical data is sparse, and modified to assess building collapse (sliding or
 513 overturning mechanism). This approach is complementary to published statistical tsunami damage
 514 fragility functions as demonstrated in the case study of Ishinomaki City.

515 To date, building damage characteristics have been treated separately from financial losses which
 516 are often of interest to policy makers and planners. This study is a first attempt to combine
 517 building damage estimations and financial losses. Using the established classification of building
 damage by MLIT,



518 building construction costs were evaluated and pegged to each damage level as replacement cost ratios.
519 The proposed replacement cost index provide an approximate estimate of potential financial losses in
520 areas where pre-existing disaster-related insurance claim settlements are lacking.

521 4.1 Main findings

522 Additional key findings emerging from this study and are summarized below:

- 523 - Analytical estimation of the potential for building collapse was calculated using building design
524 standards and accounting for resistance reduction coefficients, as well as tsunami hydrodynamic
525 force considering different debris weights. The most general case (resistance reduction coefficient
526 of 1.0 and 0 ton debris weight) yields the highest accuracy in estimating building collapse in
527 Ishinomaki city.
- 528 - Sliding alone is an insufficient explanation for building collapse. It is also important to consider
529 overturning mechanism.
- 530 - This study has confirmed that the use of maximum values for flow depth and velocity might
531 underestimate damage. Damage is likely to occur before flow depth and velocity reach maximum
532 values. The present results suggest a flow velocity of 2 m/s or more would trigger collapse for a
533 typical Japanese 2 story residential wood building
- 534 - The ratio between critical flow velocity and maximum flow velocity might be a useful alternative
535 damage intensity measure but needs further investigation – particularly in the light of intermediate
536 damage levels.
- 537 - The proposed load-resistance analysis shows higher accuracy in assessing building collapse
538 compared to previously developed fragility functions in the same study area.
- 539 - Replacement cost ratio for each level of MLIT damage classification are approximately 18%, 36%,
540 54%, 76%, 100% and 100% for damage levels 1, 2, 3, 4, 5 and 6 respectively.

541 4.2 Future applications and limitations

542 The newly proposed method can be applied globally, only where building design standards and related
543 information are known and enforced. However, such detailed analyses require higher computational
544 cost and data storage. The proposed method may only work in countries where building design codes
545 are strictly followed as in the case of Japan and for events generating heavy levels of damage.
546 Additionally, the reliability of building damage predictions using this method is dependent on the
547 accuracy of the numerical model. This depends on the availability and quality of information regarding
548 the hazard, the dominant damage mode assumed in the analysis and/or reference dataset, the assumed
549 debris weight coefficient and the resistance reduction coefficient employed. In absence of such
550 information, building damage estimates are subjected to significant uncertainty. Therefore, the
551 application of this method is not to produce absolute figures for damage estimates, but to be a useful
552 guideline for planning purposes and an alternative study for comparison.

553

554 Acknowledgments

555 This research was funded by JSPS Grant-in-Aid for Young Scientists (B) “Applying developed fragility
556 functions for the Global Tsunami Model (GTM)” (Grant No. 16K16371), JSPS-NRCT Bilateral
557 Research grant, Tokio Marine & Nichido Fire Insurance Co., Ltd., Willis Research Network (WRN)
558 and the Radchadapisek Sompoch Endowment Fund (2019), Chulalongkorn University (762003-CC).

559

560 References

- 561 1) Aida, I. (1978) Reliability of a tsunami source model derived from fault parameters, *J. Phys. Earth*, 26,
562 57–73.
- 563 2) Arikawa, T. (2009) Structural behavior under impulsive tsunami loading, *Journal of Disaster Research*,
564 4 (6), 377-381.
- 565 3) Cabinet Office of Japan (2017) Chapter 2: Damage from water-related disasters, 72 p, Available at:



- 566 http://www.bousai.go.jp/taisaku/pdf/h3003shishin_3.pdf (In Japanese) Accessed date: 28/9/2018
- 567 4) Charvet, I., Macabuag, J., and Rossetto, T.: Estimating tsunami induced building damage through
- 568 fragility functions: Critical review and research needs, *Front. Built Environ.*, 3, 1–22,
- 569 <https://doi.org/10.3389/fbuil.2017.00036>, 2017.
- 570 5) Charvet, I., Suppasri, A., Kimura, H., Sugawara, D. and Imamura, F. (2015) Fragility estimations for
- 571 Kesenuma City following the 2011 Great East Japan Tsunami based on maximum flow depths,
- 572 velocities and debris impact, with evaluation of the ordinal model's predictive accuracy, *Natural hazards*,
- 573 79(3), 2073–2099.
- 574 6) Federal Emergency Management Agency: Coastal Construction Manual (3 Vols.), 3rd edn. (FEMA 55)
- 575 (Jessup, MD, 2003).
- 576 7) Hasegawa, N., Suppasri, A., Makinoshima, F. and Imamura, F. (2018) A proposal of formula for
- 577 damage prediction of each building using actual damage data from the 2011 Great East Japan tsunami,
- 578 in *Proceedings of the Annual Conference of JSCE Tohoku branch*, II-97 (in Japanese).
- 579 8) Imamura, F. (1996) Review of tsunami simulation with a finite difference method, in H. Yeh, P. Liu,
- 580 and C. E. Synolakis (Eds.), “Long-Wave Runup Models,” pp. 25–42, Singapore: World Scientific
- 581 Publishing Co., 1996.
- 582 9) Imamura, F., Koshimura, S., Mabuchi, Y., Oie, T. and Okada, K. (2011) Tsunami simulation of the
- 583 2011 Great East Japan Tsunami using Tohoku University model (Version 1.1), available at
- 584 <http://www.tsunami.civil.tohoku.ac.jp> (In Japanese) (Accessed date: 7 November 2011)
- 585 10) Japan Building Disaster Prevention Association: Seismic evaluation (General evaluation method) Pro
- 586 Ver. 3.01, 18 pages, 2012 (In Japanese)
- 587 11) Japan Society of Civil Engineers (JSCE): Tsunami assessment method for nuclear power plants in Japan,
- 588 available at: http://www.jsce.or.jp/committee/ceofnp/Tsunami/eng/JSCE_Tsunami_060519.pdf
- 589 (Accessed date: 6 August 2016)
- 590 12) Japan Society of Material Cycles and Waste Management, Disaster Waste Countermeasure and
- 591 Reconstruction Task Team: Disaster waste classification and treatment strategy manual Version 2, the
- 592 last update on 15 June 2011, available at <http://eprc.kyoto-u.ac.jp/saigai/report/2011/04/001407.html>
- 593 (Accessed date: 14 February 2018) (In Japanese)
- 594 13) Japan Wood-Products Information and Research Center (2019) O&A on utilization of wooden materials,
- 595 Available at: <http://www.jawic.or.jp/qanda/index.php?no=19> (In Japanese) Accessed date: 28/9/2018
- 596 14) Kelman, I., & Spence, R. (2004). An overview of flood actions on buildings. *Engineering*
- 597 *Geology*, 73(3–4), 297–309.
- 598 15) Koshimura, S., Oie, T., Yanagisawa, H., and Imamura, F.: Developing Fragility Functions for Tsunami
- 599 Damage Estimation using Numerical Model and Post-Tsunami Data from Banda Aceh, Indonesia,
- 600 *Coast. Eng. J.*, 51, 243–273, 2009.
- 601 16) Latcharote, P., Suppasri, A., Yamashita, A., Adriano, B., Koshimura, S., Kai, Y. and Imamura, F.
- 602 (2017) Possible Failure Mechanism of Buildings Overturned during the 2011 Great East Japan Tsunami
- 603 in the Town of Onagawa, *Frontiers in Built Environment, Earthquake Engineering, Mega Quakes:*
- 604 *Cascading Earthquake Hazards and Compounding Risks*, 3 (16), 1–18
- 605 17) Leelawat, N., Suppasri, A., Charvet, I. and Imamura, F. (2014) Building damage from the 2011 Great
- 606 East Japan tsunami: Quantitative assessment of influential factors - A new perspective on building
- 607 damage analysis, *Natural Hazards*, 73 (2), 449–471.
- 608 18) Macabuag, J., Rossetto, T., Ioannou, I. and Eames, I. (2018) Investigation of the effect of debris-
- 609 induced damage for constructing tsunami fragility curves for building, *Geosciences* 2018, 8(4),
- 610 117.
- 611 19) Macabuag, J., Rossetto, T., Ioannou, I., Suppasri, A., Sugawara, D., Adriano, B., Imamura, F. and
- 612 Koshimura, S. (2016) A proposed methodology for deriving tsunami fragility functions for buildings
- 613 using optimum intensity measures, *Natural Hazards*, 84 (2), 1257–1285.
- 614 20) Matsutomi, H. and Harada, K.: Tsunami-trace distribution around building and its practical use, in:
- 615 *Proceedings of the 3rd International tsunami field symposium*, Sendai, Japan, 10–11 April 2010, session
- 616 3–2, 2010.
- 617 21) MN Housing and Building Laboratory (2015) Wooden house cost simulation Available at:
- 618 <http://mnsekkei-cost.blogspot.com/> (In Japanese) Accessed date: 28/9/2018
- 619 22) Mori, N., Takahashi, T. and 2011 Tohoku Earthquake Tsunami Joint Survey Group (2012) Nationwide
- 620 Post Event Survey and Analysis of the 2011 Tohoku Earthquake Tsunami, *Coastal Engineering Journal*,
- 621 54, 1250001.



- 622 23) Ministry of Land, Infrastructure, Transportation and Tourism (MLIT): Reconstruction Support
623 Survey Archive: <http://fukkou.csis.u-tokyo.ac.jp/> (Accessed date: 4 July 2012) (In Japanese)
- 624 24) Ministry of Land, Infrastructure, Transportation and Tourism (MLIT), Article 46 Enforcement
625 Ordinance of Building Standard Law:
626 25) [http://elaws.e-
627 gov.go.jp/search/elawsSearch/elaws_search/lsg0500/detail?lawId=325CO0000000338#390](http://elaws.e-gov.go.jp/search/elawsSearch/elaws_search/lsg0500/detail?lawId=325CO0000000338#390)
628 (Accessed date: 15 January 2018) (In Japanese)
- 629 26) Nadal, N. C., Zapata, R. E., Pagán, I., López, R., & Agudelo, J. (2009). Building damage due to
630 riverine and coastal floods. *Journal of Water Resources Planning and Management*, 136(3), 327-
631 336.
- 632 27) Omira, R., Baptista, M. A., Miranda, J. M., Toto, E., Catita, C., & Catalão, J. (2010). Tsunami
633 vulnerability assessment of Casablanca Morocco using numerical modelling and GIS tools. *Natural
634 Hazards and Earth Systems Sciences*, 54, 75–95.
- 635 28) Reese, S., Cousins, W. J., Power, W. L., Palmer, N. G., Tejakusuma, I. G., & Nugrahadi, S. (2007).
636 Tsunami vulnerability of buildings and people in South Java? Field observations after the July 2006
637 Java tsunami. *Natural Hazards and Earth Systems Sciences*, 7, 573–589.
- 638 29) Shoji, G. and Nakamura, T.: Damage assessment of road bridges subjected to the 2011 Tohoku
639 Pacific earthquake tsunami, *Journal of Disaster Research*, 12, 79–89, 2017.
- 640 30) Song, J., De Risi, R. and Goda, K. (2017) Influence of flow velocity on tsunami loss estimation,
641 *Geosciences* 2017, 7(4), 114.
- 642 31) Suppasri, A., Fukui, K., Yamashita, K., Leelawat, N., Ohira, H., and Imamura, F.: Developing
643 fragility functions for aquaculture rafts and eelgrass in the case of the 2011 Great East Japan
644 tsunami, *Nat. Hazards Earth Syst. Sci.*, 18, 145-155, <https://doi.org/10.5194/nhess-18-145-2018>,
645 2018.
- 646 32) Suppasri, A., Latcharote, P., Bricker, J. D., Leelawat, N., Hayashi, A., Yamashita, K.,
647 Makinoshima, F., Roeber, V., and Imamura, F.: Improvement of tsunami countermeasures based
648 on lessons from the 2011 great east japan earthquake and tsunami-Situation after five years-, *Coast.
649 Eng. J.*, 58, 1640011, <https://doi.org/10.1142/S0578563416400118>, 2016
- 650 33) Suppasri, A., Charvet, I., Imai, K. and Imamura, F.: Fragility curves based on data from the 2011
651 Great East Japan tsunami in Ishinomaki city with discussion of parameters influencing building
652 damage, *Earthquake Spectra*, Vol. 31, No. 2, 841-868, 2015.
- 653 34) Suppasri, A., Muhari, A., Futami, T., Imamura, F., and Shuto, N.: Loss functions of small marine
654 vessels based on surveyed data and numerical simulation of the 2011 Great East Japan tsunami, *J.
655 Waterway, Port, Coastal, Ocean Eng.*, 140, 04014018, [https://doi.org/10.1061/\(ASCE\)WW.1943-
656 5460.0000244](https://doi.org/10.1061/(ASCE)WW.1943-5460.0000244), 2014.
- 657 35) Suppasri, A., Koshimura, S., and Imamura, F.: Developing tsunami fragility curves based on the
658 satellite remote sensing and the numerical modeling of the 2004 Indian Ocean tsunami in Thailand,
659 *Nat. Hazards Earth Syst. Sci.*, 11, 173–189, <https://doi.org/10.5194/nhess-11-173-2011>, 2011.
- 660 36) Valencia, N., Gardi, A., Gauraz, A., Leone, F., & Guillande, R. (2011). New tsunami damage
661 functions developed in the framework of SCHEMA project: Application to European-
662 Mediterranean coasts. *Natural Hazards and Earth Systems Sciences*, 11, 2835–2846.
- 663 37) Triantafyllou, I., Novikova, T., Charalampakis, M., Fokaefs, A. and Papadopoulos, G. A. (2018)
664 Quantitative Tsunami Risk Assessment in Terms of Building Replacement Cost Based on Tsunami
665 Modelling and GIS Methods: The Case of Crete Isl., Hellenic Arc, *Pure and Applied Geophysics*
666 (Published online)
- 667 38) Yeh, H., Barbosa, A. R., Ko, H., & Cawley, J. G. (2014). Tsunami loadings on structures: Review
668 and analysis. *Coastal Engineering Proceedings*, 1(34), 4.
- 669 39) Yokohama City, Housing and Architecture Bureau: Standard weight table of wooden house and
670 standard weight table calculation basis of wooden house available at
671 <http://www.city.yokohama.lg.jp/kenchiku/shidou/shidou/toriatukai/gakeue/siryou3.pdf> (Accessed
672 date: 21 February 2018) (In Japanese)
673